Integral Equation Theory for Symmetric Nonadditive Hard Sphere Mixtures†

Kamakshi Jagannathan, Govardhan Reddy, and Arun Yethiraj*

Theoretical Chemistry Institute and Department of Chemistry, University of Wisconsin, Madison, Wisconsin 53706

Received: October 1, 2004

An integral equation theory is presented for the pair correlation functions and phase behavior of symmetric nonadditive hard sphere mixtures with hard sphere diameters given by $\sigma_{AA} = \sigma_{BB} = \lambda d$ and $\sigma_{AB} = d$. This mixture exhibits a fluid−fluid phase separation into an A-rich phase and a B-rich phase at high densities. The theory incorporates, into the closure approximation, all terms that can be calculated exactly in the density expansion of the direct correlation functions. We find that the closure approximation developed in this work is accurate for the structure and phase behavior over the entire range of λ, when compared to computer simulations, and is significantly more accurate than the previous theories.

I. Introduction

A simple but nontrivial model for describing excluded volume interactions in real fluids is a two-component mixture composed of hard spheres of unequal diameter. An additive hard sphere (AHS) mixture has the collision diameter of the unlike species, σ_{AB}, given by $\sigma_{AB} = (1/2)(\sigma_{AA} + \sigma_{BB})$, where σ_{AA} and σ_{BB} are the hard sphere diameters of species A and B, respectively. In a nonadditive hard sphere (NAHS) mixture $\sigma_{AB} \neq (1/2)(\sigma_{AA} + \sigma_{BB})$. Unlike mixtures of AHS, where a liquid−liquid phase transition is expected only for very large disparities in the sizes of the components[1,2] because of the osmotic depletion of the smaller particles in the contact region of two larger particles, NAHS mixtures with positive nonadditivity, i.e., $\sigma_{AB} > (1/2)(\sigma_{AA} + \sigma_{BB})$, readily phase separate when the density of the liquid is increased because the extra repulsion between the unlike species competes with the entropy of mixing. This mechanism of phase separation in NAHS mixtures with positive nonadditivity is used to explain the fluid−fluid phase separation in He−rare gas and He−H_2 mixtures[3,4] in extreme thermodynamic conditions of pressure and temperature. (NAHS mixtures with negative nonadditivity show a tendency toward compound formation or heterocoordination and explain the chemical short range order that is observed for some liquid alloys and amorphous mixtures.[5,6])

In this paper we present an integral equation approach to study symmetric ($\sigma_{AA} = \sigma_{BB}$) NAHS mixtures with positive nonadditivity. We consider a symmetric NAHS mixture with

$$\sigma_{AA} = \sigma_{BB} = \lambda d \quad (1)$$

$$\sigma_{AB} = d \quad (2)$$

where λ is the nonadditivity parameter. For mixtures with positive nonadditivity this model interpolates between the Widom−Rowlinson (WR) model[7] for $\lambda = 0$ and the AHS mixture for $\lambda = 1$.

Our work is partially motivated by recent semigrand ensemble Monte Carlo (MC) simulations of symmetric nonadditive mixtures,[8−10] which obtained critical densities and coexistence curves for different values of λ. These simulations,[8−10] using finite size scaling ideas, corrected earlier numerical estimates[11−15] for the critical properties, which were in significant error. Perhaps because approximations in the theories had been fine-tuned to agree with early (incorrect) simulations, none of the various theoretical approaches were found to be accurate for the location of the critical point, over the entire range of λ.[8,9] The theories tested included the MIX1 model,[11] the generalized scaled-particle theory,[16,17] the *y* expansion theory,[2,18,19] integral equation theories[8,20−23] with the Percus−Yevick (PY), hypernetted chain (HNC), Martynov−Sarkisov (MS), modified Martynov−Sarkisov (MMS), Rogers−Young (RY), and Ballone−Pastore−Galli−Gazzillo (BPGG) closures, phenomenological equations of state,[24−27] and the multiparticle correlation expansion of the configurational entropy.[28] A recent theoretical approach using the Rosenfeld functional for NAHS mixtures,[29] which performed comparisons with the recent accurate simulation results, considered values for λ ranging from 0.5 to 1. The theory presented in this work is based on the integral equation approach developed for the WR model by Yethiraj and Stell[30] (YS), where the direct correlation functions are approximated by all the terms in the density expansion that can be calculated exactly. The YS theory was significantly more accurate than the previous theories for the structure and thermodynamics of the WR fluid. In this work, we generalize the above approach to symmetric NAHS mixtures with positive nonadditivity. We consider the entire range of λ, i.e., $0 \leq \lambda \leq 0.96$. The upper limit on λ is set by the fact that the hard sphere mixture crystallizes before a fluid−fluid separation takes place.[9] We also perform calculations with the PY closure for comparison, since it is the only closure that gives convergent results for the entire range of λ. We find that the closure approximation developed in this work successfully reproduces the liquid structure and the phase behavior of symmetric NAHS mixtures when compared to simulations, for the entire range of λ.

The rest of the paper is organized as follows. The theory is described in section II, the results are presented and discussed in section III, and conclusions are presented in section IV.

II. Theory

For a binary mixture, the set of Ornstein−Zernike (OZ) equations takes the form

$$\hat{h}_{AA}(k) = \hat{c}_{AA}(k) + \rho_A \hat{c}_{AA}(k)\hat{h}_{AA}(k) + \rho_B \hat{c}_{AB}(k)\hat{h}_{AB}(k) \quad (3)$$

$$\hat{h}_{AB}(k) = \hat{c}_{AB}(k) + \rho_A \hat{c}_{AA}(k)h_{AB}(k) + \rho_B \hat{c}_{AB}(k)h_{BB}(k) \quad (4)$$

$$\hat{h}_{BB}(k) = \hat{c}_{BB}(k) + \rho_A \hat{c}_{AB}(k)\hat{h}_{AB}(k) + \rho_B \hat{c}_{BB}(k)\hat{h}_{BB}(k) \quad (5)$$

† Part of the special issue "David Chandler Festschrift".

* Corresponding author.

10.1021/jp045515h CCC: $30.25
Published on Web 12/07/2004

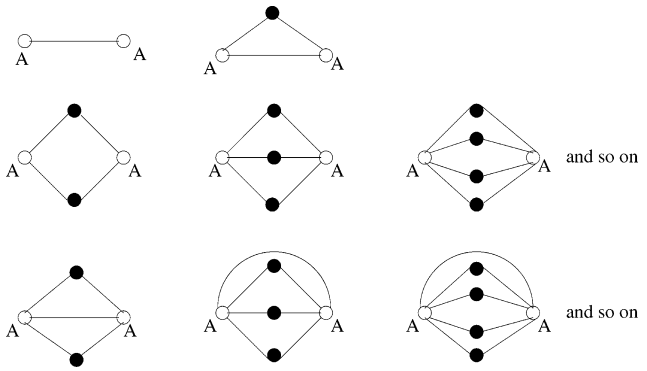

Figure 1. Diagrams that can be evaluated exactly in the expansion of the direct correlation function $c_{AA}(r)$. The solid lines in the diagrams are *f*-bonds ($f_{ij}(r) = e^{-u_{ij}(r)/k_BT} - 1$). The black circles can be either A or B. The diagrams that appear in the expansions of $c_{BB}(r)$ and $c_{AB}(r)$ are similar except that the white circles are now BB and AB, respectively.

where k is the momentum transfer variable, carets denote Fourier transforms, $h_{ij}(r)$ and $c_{ij}(r)$ are, respectively, the total and direct correlation functions between species i and j, and ρ_i is the number density of species i. The pair correlation functions are given by $g_{ij}(r) = 1 + h_{ij}(r)$. Given closure approximations between $h_{ij}(r)$ and $c_{ij}(r)$, the OZ equations can be solved to obtain the pair correlation functions and hence the thermodynamic properties. Developing closures is one of the central challenges of liquid state theory. The PY closure, in terms of the function $\gamma_{ij}(r) \equiv h_{ij}(r) - c_{ij}(r)$, is given by

$$c_{ij}(r) = [e^{-u_{ij}(r)/k_BT} - 1][1 + \gamma_{ij}(r)] \quad (6)$$

where $u_{ij}(r)$ is the interaction potential between species i and j, k_B is Boltzmann's constant, and T is the temperature.

Our approach is to include all the diagrams in the density expansion of the direct correlations that can be calculated exactly. The direct correlation function is the sum of all simple diagrams with two white 1-circles, black ρ-circles, connected by *f*-bonds, and free of connecting circles. A subset of these diagrams can be evaluated exactly, and these are shown in figure 1 for $c_{AA}(r)$. In the figure, the solid lines are *f*-bonds ($f_{ij}(r) = e^{-u_{ij}(r)/k_BT} - 1$). The black circles can be either A or B ρ-circles. The diagrams for $c_{BB}(r)$ and $c_{AB}(r)$ are similar except that the white circles become BB and AB, respectively. For hard-spheres, the *f*-functions are just Heaviside step functions, and convolution integrals involving two *f*-functions can be obtained exactly from the overlap volume of two spheres. The integrals in Figure 1 can thus be written in terms of overlap integrals $O_{AA}(r)$, $O_{AB}(r)$, and $O(r)$, which are, respectively, the volume of overlap of two spheres of diameters $2\lambda d$ and $2\lambda d$, $2d$ and

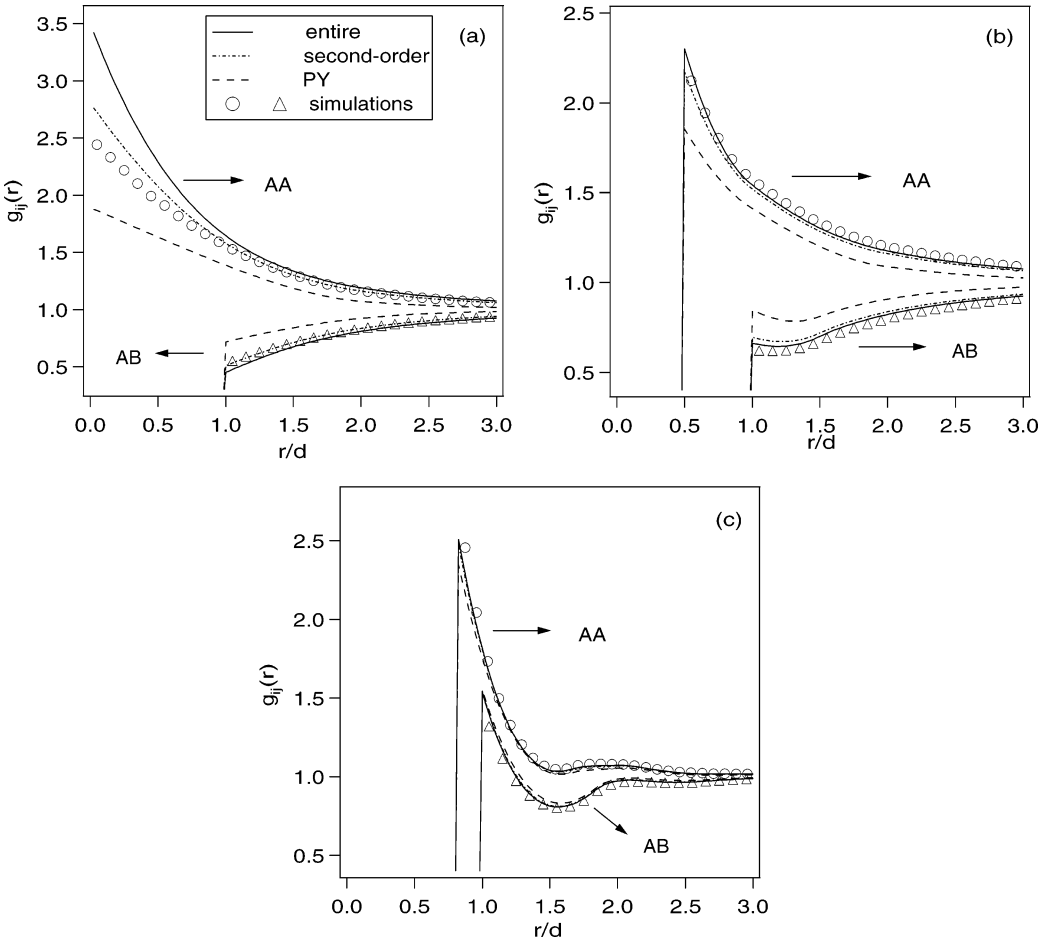

Figure 2. Comparison of the pair correlation functions from simulations (symbols) to theoretical predictions from the entire series and the second-order truncation for $\rho d^3 = 0.65$, $\phi = 0.5$, and (a) $\lambda = 0$ (WR mixture), (b) $\lambda = 0.5$, and (c) $\lambda = 0.833$. Also shown are predictions of the PY theory.

$2d$, and $2d$ and $2\lambda d$. Explicit expressions for these functions are:

$$O_{AA}(r) = O_{BB}(r) = \frac{4\pi}{3}(\lambda d)^3\left[1 - \frac{3}{2}\left(\frac{r/2}{\lambda d}\right) + \frac{1}{2}\left(\frac{r/2}{\lambda d}\right)^3\right] \quad \text{for } r < 2\lambda d$$
$$= 0 \text{ otherwise} \tag{7}$$

$$O_{AB}(r) = O_{BA}(r) = \frac{4\pi}{3}(d)^3\left[1 - \frac{3}{2}\left(\frac{r/2}{d}\right) + \frac{1}{2}\left(\frac{r/2}{d}\right)^3\right] \quad \text{for } r < 2d$$
$$= 0 \text{ otherwise} \tag{8}$$

and

$$O(r) = \frac{2\pi}{3}(d)^3\left[1 - \frac{3}{2}\left(\frac{x}{d}\right) + \frac{1}{2}\left(\frac{x}{d}\right)^3\right] + \frac{2\pi}{3}(\lambda d)^3\left[1 - \frac{3}{2}\left(\frac{y}{\lambda d}\right) + \frac{1}{2}\left(\frac{y}{\lambda d}\right)^3\right] \quad \text{for } r < \lambda d + d$$
$$= 0 \text{ otherwise} \tag{9}$$

where

$$x = \frac{r^2 + \{d^2 - (\lambda d)^2\}}{2r} \text{ and } y = \frac{r^2 - \{d^2 - (\lambda d)^2\}}{2r}$$

The diagrams in Figure 1 are summed to obtain an approximation for $c_{ij}(r)$ outside the core. The expressions for $c_{AA}(r)$, $c_{BB}(r)$, and $c_{AB}(r)$ are

$$c_{AA}(r) = -1 - (\rho_A O_{AA}(r) + \rho_B O_{AB}(r)) + e^{-u_{AA}(r)/k_BT}\left[\frac{\rho_A O_{AA}(r) e^{\rho_A O_{AA}(r)} - \rho_B O_{AB}(r) e^{\rho_B O_{AB}(r)}}{\rho_A O_{AA}(r) - \rho_B O_{AB}(r)}\right] \tag{10}$$

$$c_{BB}(r) = -1 - (\rho_B O_{BB}(r) + \rho_A O_{BA}(r)) + e^{-u_{BB}(r)/k_BT}\left[\frac{\rho_B O_{BB}(r) e^{\rho_B O_{BB}(r)} - \rho_A O_{BA}(r) e^{\rho_A O_{BA}(r)}}{\rho_B O_{BB}(r) - \rho_A O_{BA}(r)}\right] \tag{11}$$

$$c_{AB}(r) = -1 - (\rho_A O(r) + \rho_B O(r)) + e^{-u_{AB}(r)/k_BT}\left[\frac{\rho_A e^{\rho_A O(r)} - \rho_B e^{\rho_B O(r)}}{\rho_A - \rho_B}\right] \quad \text{if } \rho_A \neq \rho_B$$
$$= -1 - 2\rho_A O(r) + e^{-u_{AB}(r)/k_BT} e^{\rho_A O(r)}(1 + \rho_A O(r)) \quad \text{if } \rho_A = \rho_B \tag{12}$$

These closure relations reduce to those obtained for the WR mixture[30] for $\lambda = 0$. In this work we employ the closure in two ways: (a) by including all the terms that can be calculated exactly in the density expansion of the direct correlation functions, which is referred to as "entire series" in the rest of the paper, and (b) by including terms up to second order in density in the density expansion, referred to as "second-order truncation" in the rest of the paper. We also perform calculations with the PY closure for comparison. The exact conditions, $g_{AA}(r) = g_{BB}(r) = 0$ for $r < \lambda d$, and $g_{AB}(r) = 0$ for $r < d$, are used inside the hard core regions.

The OZ equations are solved iteratively using a standard Picard iteration procedure. An initial guess for $c_{ij}(r)$ is made and $\hat{c}_{ij}(k)$ are evaluated using the fast Fourier transform. The functions $\hat{\gamma}_{ij}(k) \equiv \hat{h}_{ij}(k) - \hat{c}_{ij}(k)$ are calculated using the OZ equations, and inverted to obtain $\gamma_{ij}(r)$. A new estimate for the $c_{ij}(r)$ is obtained by using $c_{ij}(r) = -1 - \gamma_{ij}(r)$ inside the hard core, and using the closure (e.g., equations 10−12) outside the hard core region. This estimate for the $c_{ij}(r)$ is mixed with old estimate for the $c_{ij}(r)$ to avoid numerical instabilities. The entire process is repeated until convergence. The functions are discretized with a spacing in r-space of $\Delta r = 0.025d$ and with 2^{11} points in the Fourier transform. The number of iterations required for convergence depends on the value of λ, ranging from around one hundred for $\lambda = 0$ to a few thousand for $\lambda = 0.909$.

We calculate both the spinodal and binodal curves using our theory. The spinodal curve is the locus of points where all the partial structure factors diverge and

$$\hat{\Omega}(0) \equiv 1 - \rho_A \hat{c}_{AA}(0) - \rho_B \hat{c}_{BB}(0) + \rho_A \rho_B (\hat{c}_{AA}(0)\hat{c}_{BB}(0) - \hat{c}_{AB}{}^2(0)) = 0 \tag{13}$$

The compressibility critical point occurs at the density where $\hat{\Omega}(0) = 0$. The entire spinodal curve for a particular value of λ can be obtained by calculating $\hat{\Omega}(0)$ as a function of density for different values of the composition $\phi \equiv \rho_A/\rho$.

The binodal curve is obtained via a double tangent construction to the virial free energy. For the NAHS mixture, the Helmholtz free energy, F, is given by

$$\frac{F}{Nk_BT} = \frac{F^{IG}}{Nk_BT} + \frac{F^{EX}}{Nk_BT} \tag{14}$$

where N is the total number of particles ($N = N_A + N_B$) and F^{IG} and F^{EX} are the ideal gas and excess contributions to the free energy, respectively, and are given by

$$\frac{F^{IG}}{Nk_BT} = \log(\rho\Lambda^3) - 1 + \phi\log(\phi) + (1 - \phi)\log(1 - \phi) \tag{15}$$

and

$$\frac{F^{EX}}{Nk_BT} = 2\pi\rho d^3\left[\int_0^1 d\xi\, \xi^2\{\phi^2\lambda^3 g_{AA}(\xi\lambda\sigma^+) + (1 - \phi)^2\lambda^3 g_{BB}(\xi\lambda\sigma^+) + 2\phi(1 - \phi) g_{AB}(\xi\sigma^+)\}\right] \tag{16}$$

where ρ is the total number density ($\rho = \rho_A + \rho_B$) and Λ is the thermal de-Broglie wavelength. The terms $g_{ii}(\xi\lambda\sigma^+)$ and $g_{ij}(\xi\sigma^+)$ are the contact values of the pair correlation functions in a mixture where the AA and AB hard sphere diameters are equal to $\xi\lambda\sigma$ and $\xi\sigma$, respectively. For any value of λ, the binodal curve is obtained by calculating F as a function of ϕ, at a particular value of the total density. If the minimum of F occurs for $\phi = 0.5$, that particular value of density corresponds to the one-phase region. If F has two minima, they correspond respectively to the two values of ϕ on the coexistence curve. For $\lambda = 0$, we are unable to obtain the entire binodal curve using this method, although the binodal critical density (at $\phi = 0.5$) can be calculated. Yethiraj and Stell[30] approximated $g_{AB}(r) = \exp(\gamma_{AB}(r))$ for $r > d$, instead of $g_{AB}(r) = 1 + \gamma_{AB}(r)$ (note that $c_{AB}(r) = 0$ for $r > d$), to obtain the binodal curve (there is no such approximation for $g_{AA}(r)$ and $g_{BB}(r)$). This problem, however, does not arise for any of the results presented in this paper for the other values of λ.

For comparison with the theoretical results, pair correlation functions, $g_{ij}(r)$, are calculated using canonical ensemble MC simulations using 2048 particles. The results for critical densities and coexistence curves are taken from previous semigrand

TABLE 1: Critical Densities from the Compressibility Route (spinodal) and Virial Route (binodal) Obtained Using the Closure Developed in This Work (both the entire series and the second-order truncation) and the PY Closure, for Different Values of λ Ranging from 0 to 0.909[a]

		entire series		second-order truncation		PY	
λ	simulations	spinodal	binodal	spinodal	binodal	spinodal	binodal
0	0.381 ± 0.006	0.362	0.339	0.380	0.377	0.525	0.286
0.5	0.392 ± 0.005	0.394	0.347	0.405	0.350	0.506	0.330
0.833	0.590 ± 0.005	0.655	0.576	0.661	0.578	0.706	0.576
0.909	0.740 ± 0.004	0.827	0.759	0.836	0.752	0.867	0.742

[a] The critical densities from previous semigrand ensemble MC simulations[8,9] are tabulated for comparison.

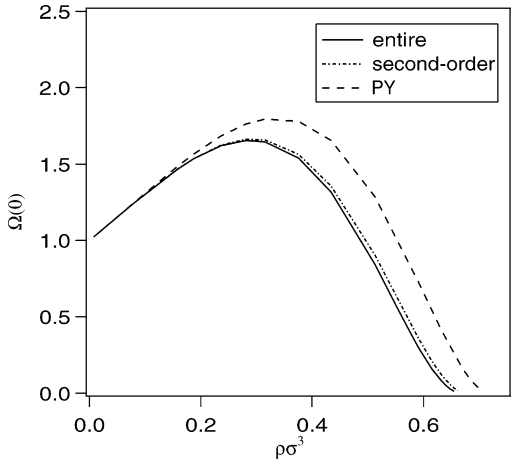

Figure 3. $\hat{\Omega}(0)$ calculated using the PY closure and the closure derived in this work (both the entire series and the second-order truncation) for $\lambda = 0.833$ and $\phi = 0.5$. The density for which $\hat{\Omega}(0) = 0$ indicates the critical density obtained from the compressibility route.

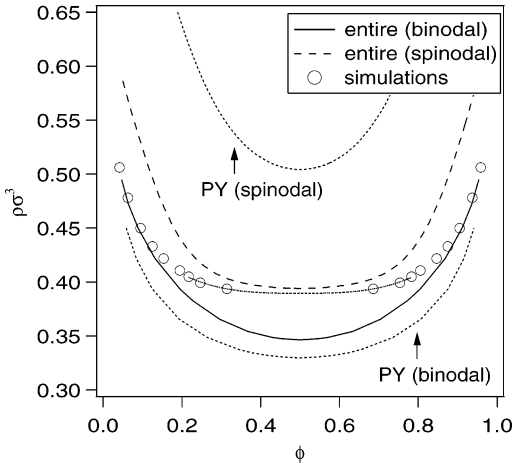

Figure 4. Binodal and spinodal curves predicted by the closure derived in this work (entire series) and the PY theory, for $\lambda = 0.5$. The symbols are simulation results[9] obtained using semigrand ensemble Monte Carlo simulations and the dotted line through the simulation results is a fit of the Ising scaling relation of the order parameter with the exponent $\beta = 0.325$ to the three state points closest to the critical point.[9]

ensemble MC simulations for NAHS mixtures.[8,9] The densities are scaled by σ^3, defined according to the one-fluid approximation as follows.[9]

$$\sigma^3 = [(\phi^2 + (1-\phi)^2)\lambda^3 + 2\phi(1-\phi)]d^3 \qquad (17)$$

III. Results and Discussion

For low values of λ, the closure obtained using the second-order truncation is quite accurate when compared to computer simulations. The closure obtained using the entire series tends to overestimate the value of $g_{AA}(r)$ and underestimate the value of $g_{AB}(r)$ near contact. The PY closure, on the other hand, tends to underestimate the value of $g_{AA}(r)$ and overestimate the value of $g_{AB}(r)$ near contact. For large values of λ, all of the closures are accurate for the pair correlation functions. These trends can be seen in Figure 2(a−c), which compares $g_{ij}(r)$ obtained using the PY closure and the closure developed in this work (both the entire series and the second-order truncation) to simulation results for $\rho d^3 = 0.65$ and $\phi = 0.5$, for $\lambda = 0$, 0.5, and 0.833, respectively. For the highest values of λ, all the theories are quantitatively accurate for $g_{ij}(r)$. The most accurate approach is the closure of the present work with the second-order truncation.

Figure 3 depicts $\hat{\Omega}(0)$ as a function of $\rho\sigma$,[3] for the PY closure and the closure developed in this work, for $\lambda = 0.833$ and $\phi = 0.5$. The compressibility route critical point occurs at the density where $\hat{\Omega}(0) = 0$.

The closure of this work is overall in better agreement with the simulations than with the PY theory. This can be seen in Figure 4, which depicts the coexistence curves (spinodal and binodal) obtained using the PY theory and the closure (entire series) of this work for $\lambda = 0.5$. Similar results are obtained with the second-order truncation, which are therefore not shown. For an exact theory, the binodal and spinodal curves meet at the critical point. This does not happen in the approximate theories considered here, because they are not thermodynamically consistent. The closure of this work shows a greater degree of thermodynamic consistency than the PY closure, i.e., the critical points obtained from the spinodal and binodal curves are closer to each other than in the PY theory.

Table 1 lists the values for the critical density from both the compressibility route (spinodal) and the virial route (binodal), for λ ranging from 0 to 0.909, using both the PY closure and the closures developed in this work. Critical densities obtained from simulations[8,9] are also shown for comparison. An exhaustive comparison of the simulation critical densities with the previous theories can be found in refs 8 and 9. First, the spinodal and binodal critical densities obtained from the closures developed in this work are closer to each other than those obtained using the PY closure, i.e., the closure of this work results in a more thermodynamically consistent theory over the entire range of λ. For lower values of λ (higher degree of nonadditivity), the closures of this work give values for critical density that are in good agreement with the simulations and are significantly more accurate than the PY theory. For high values of λ ($\lambda = 0.833$ and 0.909), the binodal critical density from both the PY closure and the closure developed in this work are nearly the same. The spinodal critical densities predicted by the closures of this work are, however, in better agreement with simulation than the PY theory.

IV. Conclusions

An integral equation theory is presented for the structure and thermodynamics of symmetric NAHS mixtures with positive

nonadditivity. The theory incorporates those terms in the density expansion of the direct correlation functions that can be evaluated exactly into the closure approximation. Theoretical predictions for the pair correlation functions, critical densities, and coexistence curves are in good agreement with the simulation results.

Acknowledgment. This material is based upon work supported by the National Science Foundation under Grant No. CHE-0315219.

References and Notes

(1) Biben, T.; Hansen, J.-P. *Phys. Rev. Lett.* **1991**, *66*, 2215.
(2) Biben, T.; Hansen, J.-P. *Physica A* **1997**, *235*, 142.
(3) Van den Bergh, L. C.; Shouten, J. A.; Trappeniers, N. J. *Physica A* **1987**, *141*, 524.
(4) Costantino, M.; Rice, S. F. *J. Phys. Chem.* **1991**, *95*, 9034.
(5) Gazzillo, D.; Pastore, G.; Enzo, S. *J. Phys.: Condens. Matter* **1989**, *1*, 3469.
(6) Gazzillo, D.; Pastore, G.; Frattini, R. *J. Phys.: Condens. Matter* **1990**, *2*, 8463.
(7) Widom, B.; Rowlinson, J. S. *J. Chem. Phys.* **1970**, *52*, 1670.
(8) Shew, C.-Y.; Yethiraj, A. *J. Chem. Phys.* **1996**, *104*, 7665.
(9) Jagannathan, K.; Yethiraj, A. *J. Chem. Phys.* **2003**, *118*, 7907.
(10) Góźdź, W. T. *J. Chem. Phys.* **2003**, *119*, 3309.
(11) Melnyk, T. W.; Sawford, B. L. *Mol. Phys.* **1975**, *29*, 891.
(12) Amar, J. *Mol. Phys.* **1989**, *67*, 739.
(13) Rovere, M.; Pastore, G. *J. Phys.: Condens. Matter* **1994**, *6*, A163.
(14) Hoheisel, C. *Phys. Rev. A* **1990**, *41*, 2076.
(15) Ehrenberg, V.; Schaink, H. M.; Hoheisel, C. *Physica A* **1990**, *169*, 365.
(16) Tenne, R.; Bergmann, E. *Phys. Rev. A* **1978**, *17*, 2036.
(17) Mazo, R.; Bearman, R. J. *J. Chem. Phys.* **1990**, *93*, 6694.
(18) Barboy, B.; Gelbart, W. N. *J. Chem. Phys.* **1979**, *71*, 3053.
(19) Barboy, B.; Gelbart, W. N. *J. Stat. Phys.* **1980**, *22*, 709.
(20) Nixon, J. H.; Silbert, M. *Mol. Phys.* **1984**, *52*, 207.
(21) Ballone, P.; Pastore, G.; Galli, G.; Gazzillo, D. *Mol. Phys.* **1986**, *59*, 275.
(22) Gazzillo, D. *J. Chem. Phys.* **1991**, *95*, 4565.
(23) Lomba, E.; Alvarez, M.; Lee, L. L.; Almarza, N. E. *J. Chem. Phys.* **1996**, *104*, 4180.
(24) Jung, J.; Jhon, M. S.; Ree, F. H. *J. Chem. Phys.* **1994**, *100*, 9064.
(25) Jung, J.; Jhon, M. S.; Ree, F. H. *J. Chem. Phys.* **1995**, *102*, 1349.
(26) Hamad, E. Z. *J. Chem. Phys.* **1996**, *105*, 3222.
(27) Hammawa, H.; Hamad, E. Z. *J. Chem. Soc., Faraday Trans.* **1996**, *92*, 4943.
(28) Saija, F.; Pastore, G.; Giaquinta, P. V. *J. Phys. Chem. B* **1998**, *102*, 10368.
(29) Schmidt, M. *J. Phys.: Condens. Matter* **2004**, *16*, L351.
(30) Yethiraj, A.; Stell, G. *J. Stat. Phys.* **2000**, *100*, 39.